Journal of Molecular Structure 1199 (2020) 126980

Contents lists available at ScienceDirect

Journal of Molecular Structure

journal homepage: http://www.elsevier.com/locate/molstruc

Iodine mediated rearrangement of tetraarylpiperidin-4-ones: Synthesis, structure analysis and biological studies of 5-aryl-2-methoxy-2,4-diphenyl-1*H*-pyrrole-3-ones

G. Vengatesh [a], M. Sundaravadivelu [a, *], S. Muthusubramanian [b]

[a] Department of Chemistry, The Gandhigram Rural Institute (Deemed to Be University), Gandhigram, 624302, Tamil Nadu, India
[b] Department of Organic Chemistry, School of Chemistry, Madurai Kamaraj University, Madurai, 625 021, Tamil Nadu, India

ARTICLE INFO

Article history:
Received 25 May 2019
Received in revised form
22 August 2019
Accepted 22 August 2019
Available online 26 August 2019

Keywords:
Iodine/MeOH
Ring contraction rearrangement
Pyrrole
2D NMR
X-ray-diffraction
Biological activity

ABSTRACT

An interesting iodine/methanol mediated rearrangement of tetraaylpiperidin-4-ones to 2-methoxy-2,4,5-triaryl-1*H*-pyrrole-3-ones is described. The structural features of the products are investigated by spectral data and single crystal X-ray analysis. The antifungal, antibacterial and antioxidant characteristics of the synthesized compounds have been studied.

1. Introduction

In recent years, the molecular iodine finds immense applications in various organic reactions [1–3]. It is widely available, less toxic, relatively inexpensive and stable towards air and moisture. Iodine in methanol has been used as a successful reagent for the transformation of cyclic compounds to aromatic compounds and has been extensively used in the last decade [4–10]. Iodine mediated reactions have resulted in the formation of new C–C, C–O, C–N and N–S bonds [11–16]. Iodine and methanol play vital role in the one-pot four-component domino reaction towards the synthesis of substituted dihydro-2-oxypyrroles [17], in the one-pot synthesis of flavanone and tetrahydro pyrimidine derivatives via Mannich type reaction [18] and in the synthesis of 2,3-disubstituted furopyridines *via* electrophilic cyclization of *o*-acetoxy and *o*-benzyloxyalkynylpyridines [19].

The nitrogen heterocyclic compounds have great importance because of their profound application in material and biological systems [20–22]. Among the nitrogen heterocyclic compounds, pyrrole is one of the most popular core units in many natural products and more than hundred marketed drugs have pyrrole moiety in their skeleton. Pyrrole derivatives also act as building blocks for various biologically active molecules and functional materials [23]. Many alkaloids and amino acids contain the reduced pyrrole ring [24]. Pyrrole derivatives exhibit anti-microbial [25], anti-viral [26], antitumor [27], antitubulin [28], antimalarial [29] and anticancer activities [30–32]. Examples of drug molecules containing pyrrole cores are given in Fig. 1.

In an attempt to get tetrasubstituted symmetrical pyridine, the dehydrogenation of tetraaryl piperidone was aimed at, wherein an interesting rearrangement has occurred resulting in dihydropyrrole derivative. The course of this reaction, the structure analysis and the biological application of the pyrrole derivatives are described in this article.

2. Experimental

2.1. Materials and methods

The progress of the reactions was monitored by TLC and the crude compounds have been purified by column chromatography on silica gel 60–120 mesh (hexane: ethyl acetate). Melting points

* Corresponding author.
E-mail address: msundargri@gmail.com (M. Sundaravadivelu).

https://doi.org/10.1016/j.molstruc.2019.126980
0022-2860/

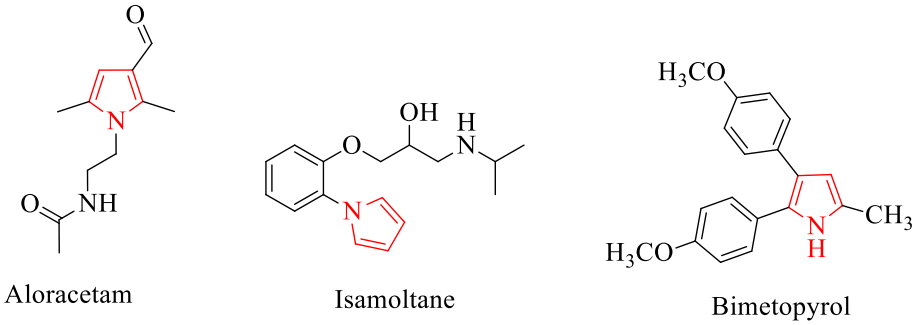

Fig. 1. Pyrrole cores containing drugs.

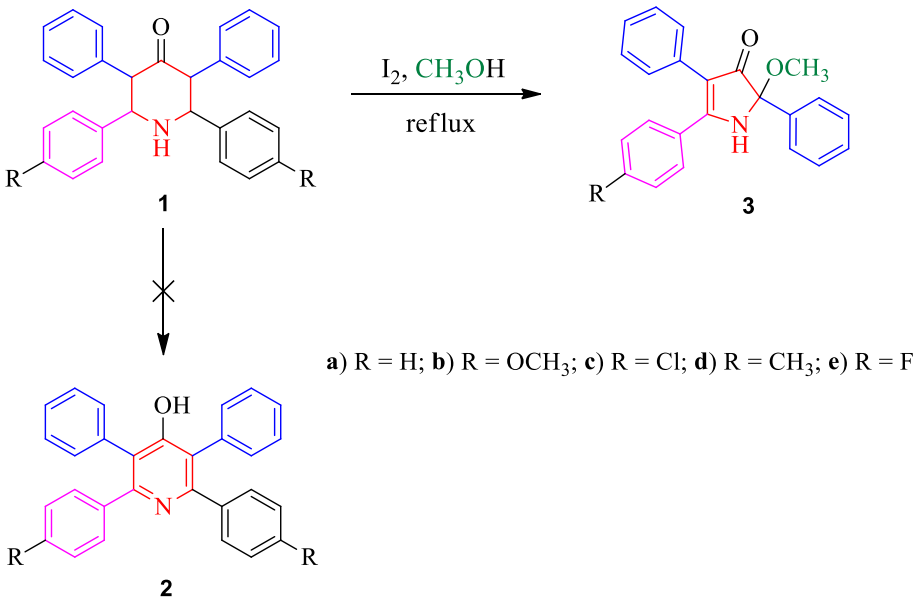

Scheme 1. Synthesis of 5-aryl-2-methoxy-2,4-diphenyl-1*H*-pyrrol-3-ones **3**.

were determined by the open capillary method. FT−IR spectra were recorded with a JASCO FT/IR−4700 spectrometer using KBr pellets. NMR spectra were recorded at 400 MHz with a Bruker AVANCE III HD spectrometer. Chemical shifts are reported in δ (ppm) scale relative to TMS as internal standard. The compound (2 mg) was dissolved in 0.5 ml of DMSO/d_6 and used to measure the ^{1}H NMR chemical shift. To record ^{13}C NMR, DEPT-135, ^{1}H−^{1}H COSY, NOESY, HSQC, HMBC NMR spectra, 20 mg of the samples was used. Single crystal structure data of compound **3e** was collected by Bruker Smart Apex II Diffractometer. Powder XRD data of compounds **3a-3e** were recorded by PANalytical X'pert3 powder X-ray Diffractometer.

2.2. Antimicrobial studies

Compounds **3a-3e** were screened for their *in vitro* antibacterial and antifungal activities. They were screened against three Gram-positive bacterial strains - *Staphylococcus aureus, Bacillus cereus* and *Enterococcus faecalis* - and one Gram-negative bacterial species - *Klebsiella pneumoniae*. The antifungal activity was assessed against *Candida albicans*. Streptomycin (for bacterial activity) and Nystatin (for fungal activity) were used as the references. The antioxidant activity was studied by DPPH method.

2.3. Typical experimental procedure for the synthesis of compounds *3a-3e*

Reactants **1a-1e** were prepared by modified Mannich condensation by Nollar-Balaiah method. 3,5-diphenyl-2,6-diaryl piperidine-4-one (**1**) (1 mmol) and iodine (2 mmol) were dissolved in 10 ml of methanol and the mixture was heated at 70 °C for 5 h. The reaction mixture was cooled and the solvent evaporated under vacuum to obtain the yellow colour product **3**. The crude product **3e** was recrystalized from methanol by solvent evaporation method.

2.3.1. 2-Methoxy-2,4,5-triphenyl-1H-pyrrol-3-one (*3a*)

melting point (mp) 219 °C. **UV:** 382 nm. **FT-IR**: 3266, 1670 cm^{-1}.**^{1}H-NMR** (400 MHz, DMSO): δ 7.06 (2H, d, J = 7.20 Hz), 7.11 (2H, t, J = 7.20 Hz), 7.19 (2H, t, J = 7.52 Hz), 7.35−7.42 (3H, m), 7.47−7.56 (5H, m), 7.60 (2H, d, J = 8.04 Hz), 9.11 (1H, s). **^{13}C-NMR** (100 MHz, DMSO): δ 51.6, 91.8, 107.6, 126.1, 126.2, 128.4, 128.8, 128.8, 128.9, 129.2, 131.2, 132.1, 132.2, 137.6, 174.3, 196.9.

2.3.2. 2-Methoxy-5-(4-methoxyphenyl)-2,4-diphenyl-1H-pyrrol-3-one (*3b*)

mp 249 °C. **UV:** 381 nm. **FT-IR**: 3258, 1662 cm^{-1}.**^{1}H-NMR** (400 MHz, DMSO): δ 3.33 (s, 3H), 3.82 (s, 3H), 7.05 (2H, d, J = 8.04 Hz), 7.09 (2H, d, J = 7.32 Hz), 7.15 (1H, t, J = 7.16 Hz), 7.23 (2H, t, J = 7.68 Hz), 7.35−7.41 (3H, m), 7.51 (2H, d, J = 6.96 Hz), 7.57

Table 1
Yield and melting point of the synthesized compounds **3**.

Entry	Substrates (1)	Products (3)	Yield (%)	mp° C
1	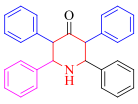 **1a**	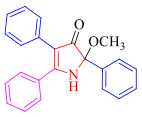 **3a**	82	219
2	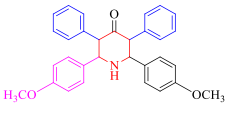 **1b**	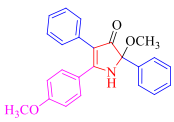 **3b**	88	249
3	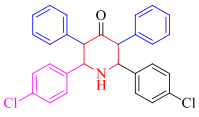 **1c**	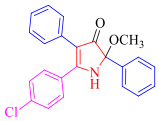 **3c**	80	244
4	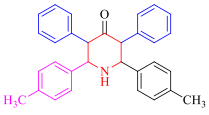 **1d**	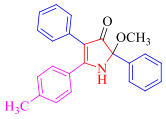 **3d**	83	213
5	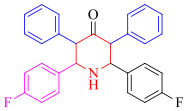 **1e**	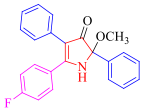 **3e**	76	233

(2H, d, $J = 7.76$ Hz) 8.94 (1H, s). **^{13}C-NMR** (100 MHz, DMSO): δ 51.6, 55.9, 91.8, 107.0, 114.6, 122.9, 126.1, 126.2, 128.4, 128.8, 129.4, 130.9, 132.7, 137.8, 162.3, 173.7, 196.4.

*2.3.3. 5-(4-Chlorophenyl)-2-methoxy-2,4-diphenyl-1H-pyrrol-3-one (**3c**)*

mp 244 °C. **UV:** 386 nm. **FT-IR**: 3263, 1665 cm^{-1}.**^{1}H-NMR** (400 MHz, DMSO): δ 3.33 (s, 3H), 7.07 (2H, d, $J = 7.20$ Hz), 7.14 (1H, t, $J = 6.80$ Hz), 7.22 (2H, t, $J = 6.80$ Hz), 7.36–7.42 (3H, m), 7.52 (2H, d, $J = 6.40$ Hz), 7.59 (4H, s) 9.12 (1H, s). **^{13}C-NMR** (100 MHz, DMSO): δ 51.7, 91.8, 107.9, 126.2, 126.3, 128.5, 128.8, 128.9, 129.2, 129.3, 129.9, 130.8, 131.9, 136.8, 137.3, 172.9, 196.9.

*2.3.4. 2-Methoxy-2,4-diphenyl-5-(p-tolyl)-1H-pyrrol-3-one (**3d**)*

mp 213 °C. **UV:** 383 nm. **FT-IR**: 3256, 1668 cm^{-1}.**^{1}H-NMR** (400 MHz, DMSO): δ 2.37 (s, 3H), 3.33 (s, 3H), 7.07 (2H, d, J = 6.80), 7.12 (1H, t, $J = 7.60$ Hz), 7.21 (2H, t, $J = 7.20$ Hz), 7.29 (2H, d, $J = 8.00$ Hz), 7.35–7.41 (3H, m), 7.48–7.525 (4H, m) 9.02 (1H, s). **^{13}C-NMR** (100 MHz, DMSO): δ 21.6, 51.6, 91.8, 107.3, 126.1, 126.2, 128.2, 128.3, 128.8, 128.9, 129.3, 129.8, 132.4, 137.7, 142.2, 174.2, 196.7.

*2.3.5. 5-(4-Fluorophenyl)-2-methoxy-2,4-diphenyl-1H-pyrrol-3-one (**3e**)*

mp 233 °C. **UV:** 383 nm. **FT-IR**: 3263, 1665 cm^{-1}.**^{1}H-NMR** (400 MHz, DMSO): δ 3.34 (s, 3H), 7.07 (2H, d, $J = 7.20$ Hz), 7.13 (1H, t, $J = 7.32$ Hz), 7.22 (2H, t, $J = 7.60$ Hz), 7.34–7.42 (5H, m), 7.53 (2H, d, $J = 7.60$ Hz), 7.67 (2H, t, $J = 8.64$ Hz) 9.10 (1H, s). **^{13}C-NMR** (100 MHz, DMSO): δ 51.6, 91.8, 107.8, 116.3, 126.3, 127.5, 128.5, 128.8, 128.9, 129.3, 131.7, 132.1, 137.5, 164.2, 173.1, 196.8; *m/z*: calcd. for $C_{23}H_{18}FNO_2$ 359.132; found 359.118. anal. calcd. For $C_{23}H_{18}FNO_2$: C, 81.59, N, 8.63, H, 9.78. Found: C, 82.19, N, 8.98, H, 7.40.

3. Results and discussion

Iodine in methanol is found to be effective in the aromatization of carbo and heterocyclic rings [7]. In an attempt to dehydrogenate tetraaryl substituted piperidin-4-one to pyridine-4-ol (**2**), the oxidative aromatization of 2,3,5,6-tetraarylpiperidin-4-one (**1**) was aimed employing iodine and methanol. It was anticipated that the presence of four aryl groups could drive the piperidone ring to complete aromatization providing conjugation delocalizing the

Table 2
^{1}H NMR chemical shift value of compounds **3a-3e**.

Compounds	Aliphatic			Aromatic ring **A**			Aromatic ring **B**			Aromatic ring **C**		
	N–H	OCH_3	Others	Ortho	Meta	para	Ortho	Meta	para	Ortho	Meta	para
3a	9.11	3.34	–	7.06	7.19	7.11	7.47–7.53		7.42	7.60	7.37	4.56
3b	8.94	3.33	3.82	7.09	7.23	7.13	7.51	7.35–7.41		7.57	7.05	–
3c	9.12	3.33	–	7.07	7.22	7.15	7.52	7.36–7.42		7.59		–
3d	9.02	3.33	2.37	7.07	7.31	7.12	7.50	7.38	7.41	7.52	7.21	–
3e	9.10	3.34	–	7.07	7.24	7.13	7.53	7.40	7.42	7.64–7.67	7.36	–

Table 3
^{13}C NMR chemical shift value of compound **3a-3e**.

Compounds	C2	C3	C4	C5	CH_3
3a	91.8	196.9	107.6	174.3	51.6
3b	91.8	196.4	107.0	173.7	51.6
3c	91.8	196.9	107.9	172.9	51.7
3d	91.8	196.7	107.3	174.2	51.6
3e	91.8	196.8	107.8	173.1	51.6

Compounds	Aromatic ring **A**				Aromatic ring **B**				Aromatic ring **C**			
	ipso	ortho	meta	para	ipso	ortho	meta	para	ipso	ortho	meta	para
3a	137.5	129.2	128.9	126.2	132.0	129.2	128.8	126.2	132.2	131.1	128.3	126.1
3b	137.8	129.4	128.7	126.2	132.7	129.4	128.4	126.1	122.9	130.9	114.5	162.3
3c	137.3	129.3	128.8	126.3	131.9	129.2	128.5	126.3	129.9	130.6	126.2	136.7
3d	137.7	129.3	128.7	126.2	132.4	128.9	128.4	126.2	132.4	129.7	128.4	142.3
3e	137.4	129.3	128.4	126.3	132.0	126.2	128.9	126.3	127.5	131.6	116.3	164.2

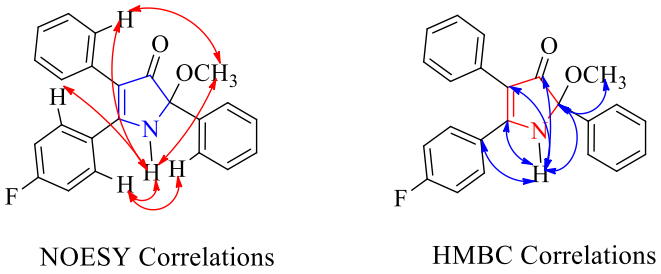

Fig. 2. Important NOESY and HMBC correlations.

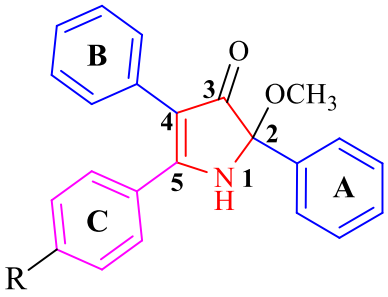

Fig. 3. Atom numbering of compound **3**.

pyridyl ring electrons, in spite of the probable nonplanarity. The reaction was carried out with 200 mol percent of iodine in methanol. The product obtained has been shown to be 2,4,5-triaryl-2-methoxy-1H-pyrrol-3-one (**3**) (*vide infra*) instead of the expected 3,5-diphenyl-2,6-diaryl pyridin-4-ol (Scheme 1). Obviously, iodine mediated ring contraction has occurred incorporating methoxy group from the solvent, methanol. The reaction has been carried out with differently substituted piperidones with very good yield (Table 1). In fact, there was no need for any optimization of the reaction conditions to improve the yield or conditions. Tables 2 and 3 provide the NMR spectral features of compounds **3a-3e**. The unambiguous structural proof for **3** has been provided by the two-dimensional NMR data and the single crystal X-ray analysis of one of the compounds, **3e**. Important NOESY and HMBC correlations are shown in Fig. 2. Atom numbering of the compound **3** is given in Fig. 3 for ^{1}H and ^{13}C NMR chemical shift identification. The features of single crystal X-ray studies are described below.

3.1. Single crystal XRD studies

3.1.1. Structural commentary

An ORTEP view of the compound **3e** is shown in Fig. 4 and data collection, structure refinement details are summarized in Table 4. The crystal is orthorhombic with *Aba*2 space group with eight molecules in the unit cell. The C12–C17 phenyl rings are almost orthogonal to the central pyrrole ring, with dihedral angle 75.94°. The phenyl and fluorophenyl rings are inclined to the central pyrrole ring at angles of 45.88° for C18–C23 and 33.86° for C1–C6. Probably due to the steric repulsion between the adjacent phenyl and fluorophenyl rings, the dihedral angle is increased to 54.90°. The central pyrrole ring containing phenyl, fluorophenyl rings and methoxy group is not in the co-planar arrangement, the N1–C10–C12–C13, N1–C10–O3–C11, C9–C8–C18–C23 and N1–C7–C3–C4 torsion angles being −19.37, 64.57, −49.38 and −30.94, respectively.

3.1.2. Supramolecular features

In the crystal, the molecules are linked by hydrogen bonding (N1–H1···O2, C11–H11···F and C16–H16···F) and C–H … π stacking (C17–H17 … Cg4 and C23–H23 … Cg2) interactions (Figs. 5 and 6). The shortest intermolecular hydrogen bond contact is N1–H1···O2 (Table 1), which joins the molecules into an infinite ribbon with graph-set motif C(9) along the b-axis direction (Fig. 5) [33]. Two such adjacent hydrogen-bonded ribbons are connected to each other *via* bifurcated C11–H11···F and C16–H16···F hydrogen

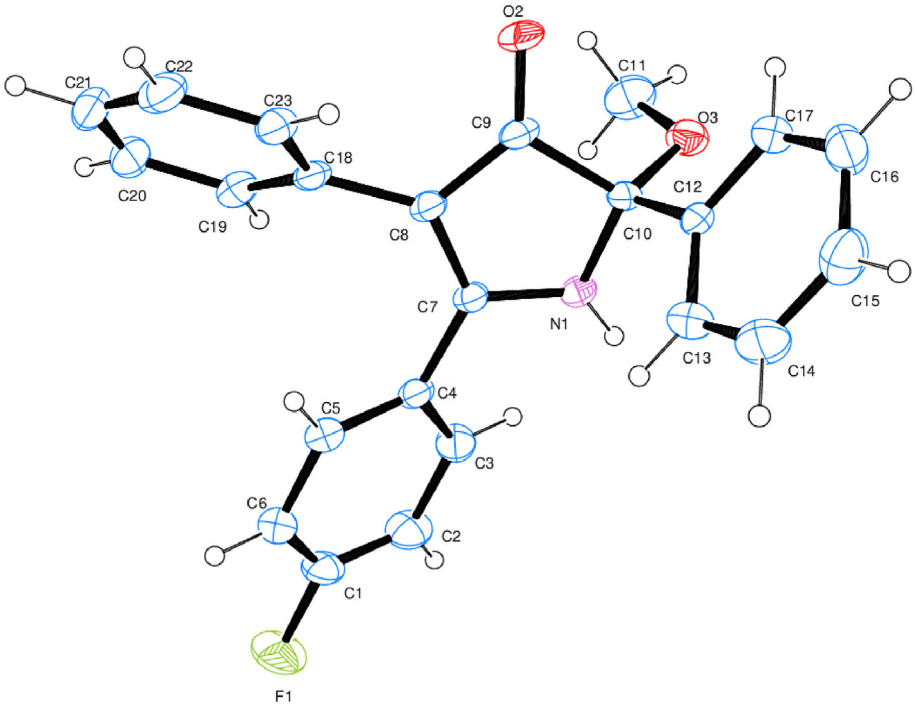

Fig. 4. ORTEP view of the compound **3e**.

Table 4
Crystallographic data for and structure refinement parameters for compound **3e**.

Crystal data	
Chemical formula	$C_{23}H_{18}FNO_2$
M_r	359.38
Crystal system, space group	Orthorhombic, *Aba*2
Temperature (K)	296
a, *b*, *c* (Å)	19.6547 (9), 12.5104 (6), 15.1399 (6)
V (Å^3)	3722.7 (3)
Z	8
Radiation type	Mo *Kα*
μ (mm^{-1})	0.09
Crystal size (mm)	0.35 × 0.30 × 0.20
Data collection	
Diffractometer	Bruker AXS Kappa Apex2 CMOS diffractometer
Absorption correction	Multi-scan *SADABS* (Bruer, 1999)
T_{min}, T_{max}	0.92, 0.96
No. of measured, independent and observed [$I > 2\sigma(I)$] reflections	16900, 4845, 3445
R_{int}	0.051
$(\sin\theta/\lambda)_{max}$ (Å^{-1})	0.683
Refinement	
$R[F^2 > 2\sigma(F^2)]$, w$R(F^2)$, *S*	0.059, 0.115, 1.14
No. of reflections	4845
No. of parameters	247
No. of restraints	1
H-atom treatment	H-atom parameters constrained
$\Delta\rho_{max}$, $\Delta\rho_{min}$ (e Å^{-3})	0.26, −0.19
Absolute structure	Refined as an inversion twin.
Absolute structure parameter	0.6 (15)

bonding and C17—H17 … Cg4 and C23—H23 … Cg2 stacking interactions (Table 5, Fig. 5). Intramolecular stacking interactions are observed between the acceptor pyrrole ring (N1/C7—C10) and adjacent C11—H11B, C11—H11C and C13—H13 donor atoms (Fig. 6).

3.1.3. Hirshfeld surface analysis

Hirshfeld surface analysis serves as a powerful tool for gaining additional insight into intermolecular interactions of molecular crystals. Hirshfeld surfaces and fingerprint plots were generated for the title compound using Crystal Explorer [34,35]. On the Hirshfeld surface mapped over d_{norm} in Fig. 7, the red colour indicates distance shorter (in close contact) than the van der Waals radii. The white colour indicates contacts with distances equal to the sum of van der Waals radii and the blue colour indicates contacts with distances longer (distinct contact) than the van der Waals radii. In Fig. 7, the interactions are characterized as the bright-red spots near the nitrogen and oxygen, the diminutive-red sport near to Cg4 (C18—C23) phenyl ring. These indicate donor and acceptor roles in the dominant N—H···O hydrogen bonding and C—H … π stacking interaction contacts. The overall two-dimensional fingerprint plot and those delineated into H···H, C···H/H···C, F···H/H···F, H···O/O···H, C···F/F···C contacts are illustrated in Fig. 8. The most important interaction, H···H contributing 51.5% to the overall crystal packing, is reflected as widely scattered points of high density due to the large hydrogen content of the molecule. The shorter hydrogen bonding interaction N—H···O is contributing 9.4% to the overall crystal packing. The bifurcated C—H···F hydrogen bonding interaction is contributing 9.5% to the overall crystal

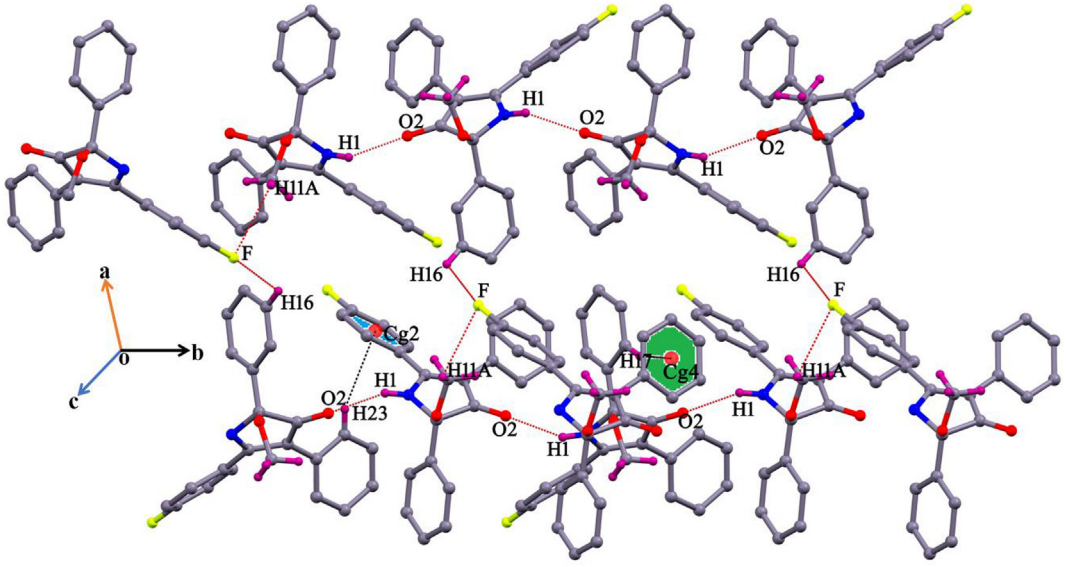

Fig. 5. A packing diagram of the compound **3e**, showing a C(9) chain to the b axis formed via N—H···O hydrogen bond, bifurcated C—H···F and C—H … π interactions.

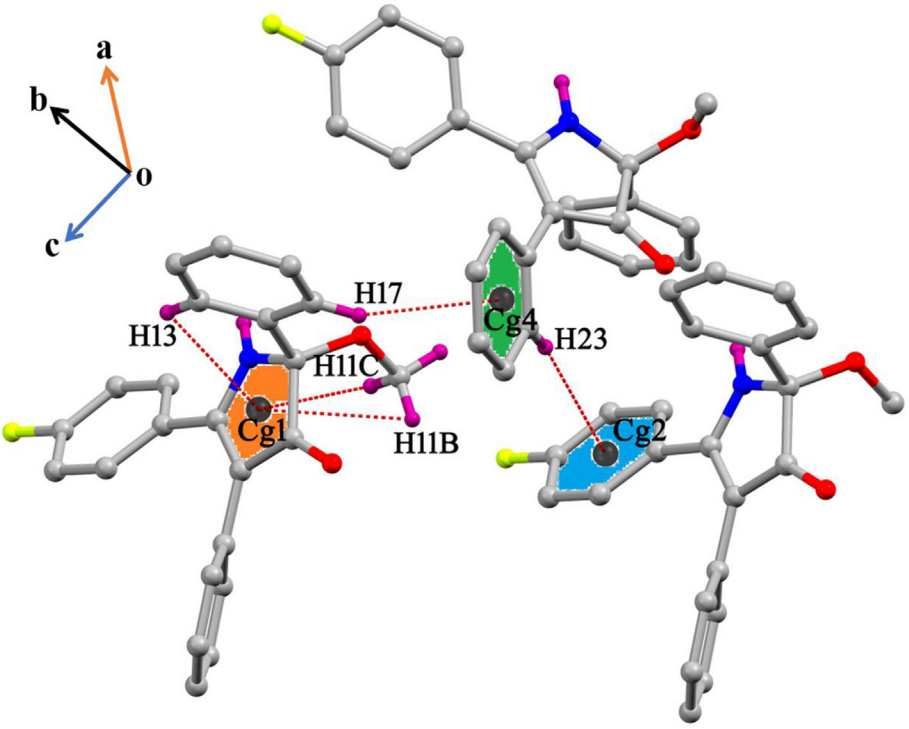

Fig. 6. Intramolecular and Intermolecular C–H … π interactions.

Table 5
Hydrogen-bond geometry (Å,°) Cg1, Cg2 and Cg4 are the centroids of the major and minor components of the N1/C7–C10, C1–C6 and C18–C23 rings, respectively.

D–H … A	D–H	H … A	D … A	D–H … A
N–H1···O2^{i}	0.86	2.19	2.910 (3)	141
C11–H11A … F^{ii}	0.96	2.87	3.166	165
C16–H16 … F^{iii}	0.93	2.66	3.187	116
C11–H11B … Cg1^{iv}	0.95	2.99	2.879(5)	74
C11–H11C … Cg1^{iv}	0.95	2.66	2.879(5)	93
C13–H13 … Cg1^{iv}	0.93	2.81	3.007(4)	93
C17–H17 … Cg4^{v}	0.93	2.83	3.688(4)	154
C23–H23 … Cg2^{vi}	0.93	2.98	3.864(4)	159

Symmetry codes: (i) 3/2-x,1/2 + y,z; (ii) −1/2 + x,1-y,-1/2 + z; (iii) x,1/2 + y,1/2 + z; (iv) X,Y,Z; (v) 3/2-X,Y,-1/2 + Z; (vi) 3/2-X,-1/2 + Y,Z.

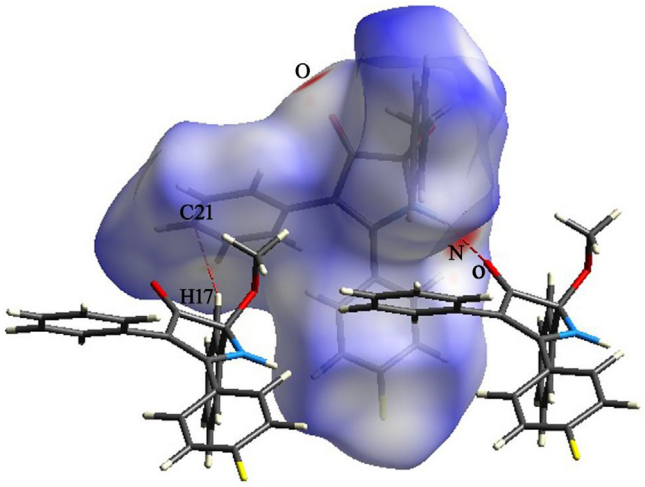

Fig. 7. The Hirshfeld surface mapped over d_{norm}, showing intermolecular interactions.

packing. The C···H/H···C interactions contribute 26.3% and weak C···F/F···C intermolecular interactions contribute 1.2% to the overall crystal packing.

3.2. Power XRD analysis

It was tried to crystallize all the compounds, but compound **3e** alone provided crystals suitable for single crystal X-ray analysis. The crystalline nature of the compounds **3a-3e** was confirmed by power XRD studies. The comparison of the powder XRD (PXRD) pattern and single crystal XRD (SCXRD) pattern of the compound **3e** is shown in Fig. 9. The sharp pattern of PXRD clearly suggests the crystalline nature of compound **3e**. In Fig. 9, large number of the 2θ values are coinciding with PXRD and SCXRD results indicating a similar pattern in both PXRD and SCXRD studies. The coinciding 2θ values of both the experiments and the comparison of PXRD patterns of compounds **3a-3e** are given in the supporting information.

3.3. Mechanism

To provide a convincing mechanism for the conversion of piperidone **1** to pyrrole-3-one **3** by the treatment of iodine in methanol, a control experiment has been carried out (Scheme 2). It has been shown that the presence of aryl groups at 3 and 5 positions of the piperidone is important for this reaction. Though enough experimental proof is not there, a tentative mechanism for the conversion of the piperidone **1** to pyrrole-3-one **3** by the treatment of iodine in methanol can be visualized as shown in Scheme 3.

Normally halogenation at alpha position through enol intermediate is the course of reaction for any halogen treatment with active methylene system. But here, before the iodide counter ion attacks the alpha position, internal nucleophilic attack would have taken place by nitrogen generating a three membered intermediate. The charged unstable three membered gets cleaved through

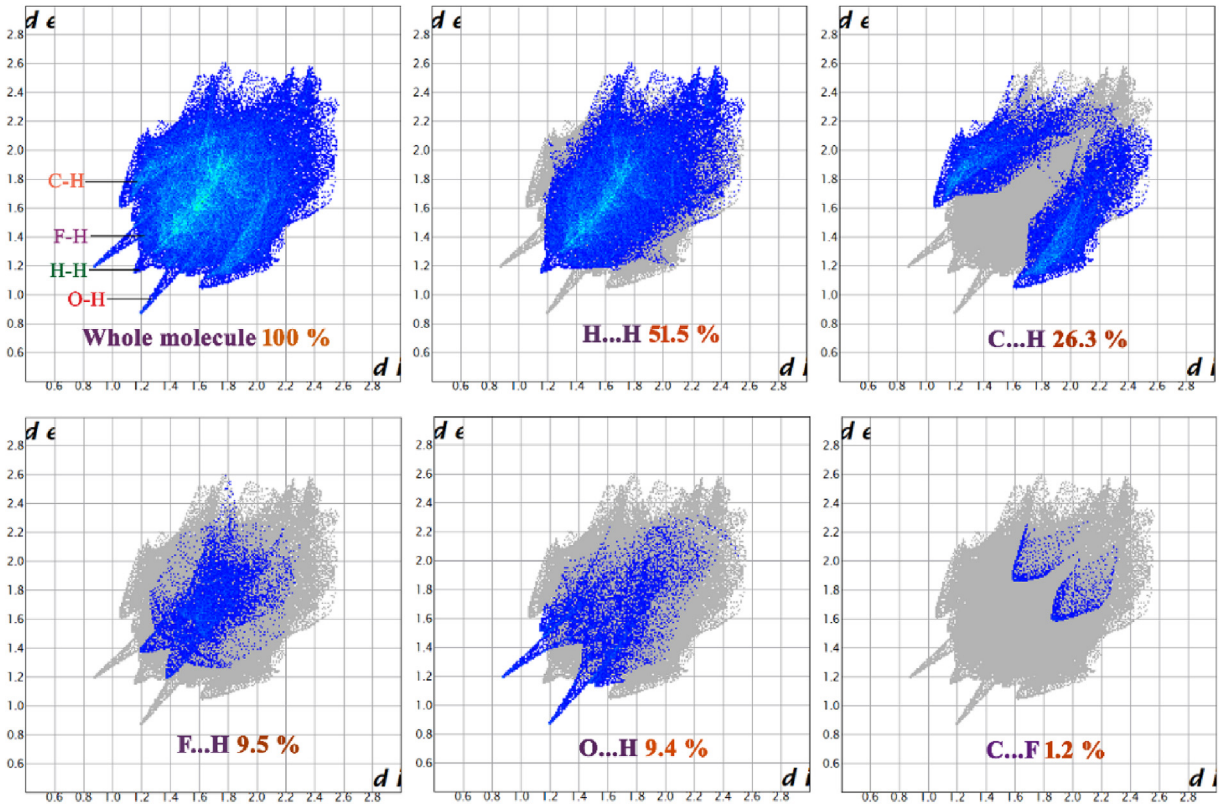

Fig. 8. Two-dimensional fingerprint plots for the compound.

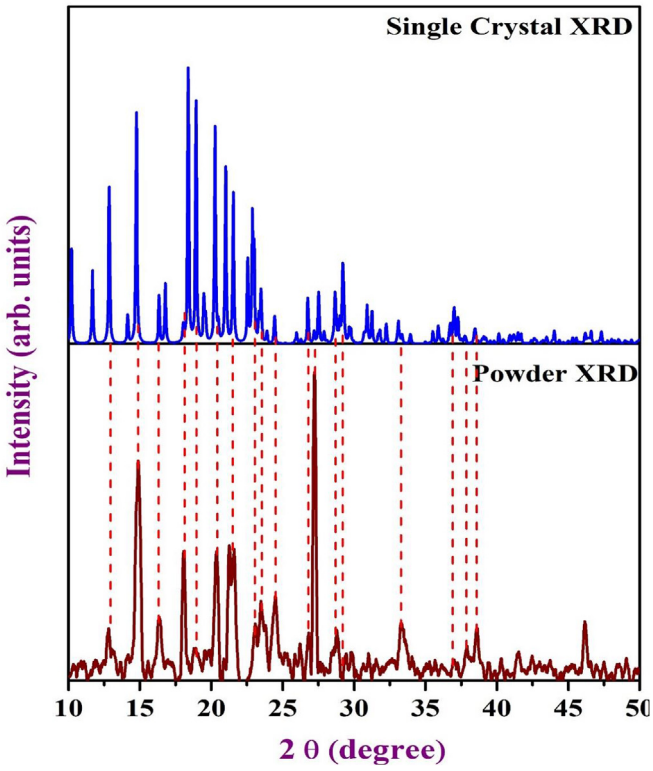

Fig. 9. Comparison of powder XRD and single crystal XRD patterns of compound **3e**.

internal nucleophilic substitution, iodide being the nucleophile and positively charged nitrogen being the leaving group. Now methanol might have attacked the alpha carbon, which is electron deficient. Another nucleophilic substitution could have occurred, now methanol is the nucleophile and benzyl anion is the leaving group. Benzyl anion is stable enough and that may be the driving force for kicking it out. Subsequent dehydrogenation by iodine, which is popular, might have led to the product **3**. The presence of aryl at 3 and 5 positions are required to stabilize the cation **B** and for the solvolysis reaction at the tertiary carbon of **G.**

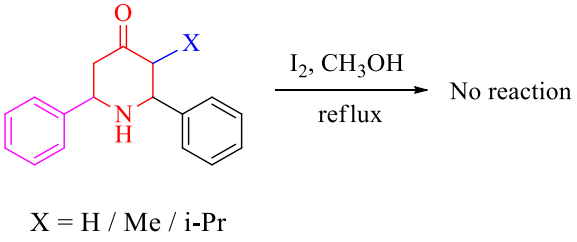

Scheme 2. Control experiment.

3.4. Biological activity

As pointed out in the introduction, many dihydropyrrole derivatives are found to be biologically active. Hence the antifungal, antibacterial and antioxidant characteristics of the prepared pyrrole derivatives **3** have been investigated and the results are presented here.

3.4.1. Antifungal activity

All the synthesized compounds were tested for their *in vitro* antifungal activity against *Candida albicans* and the results are

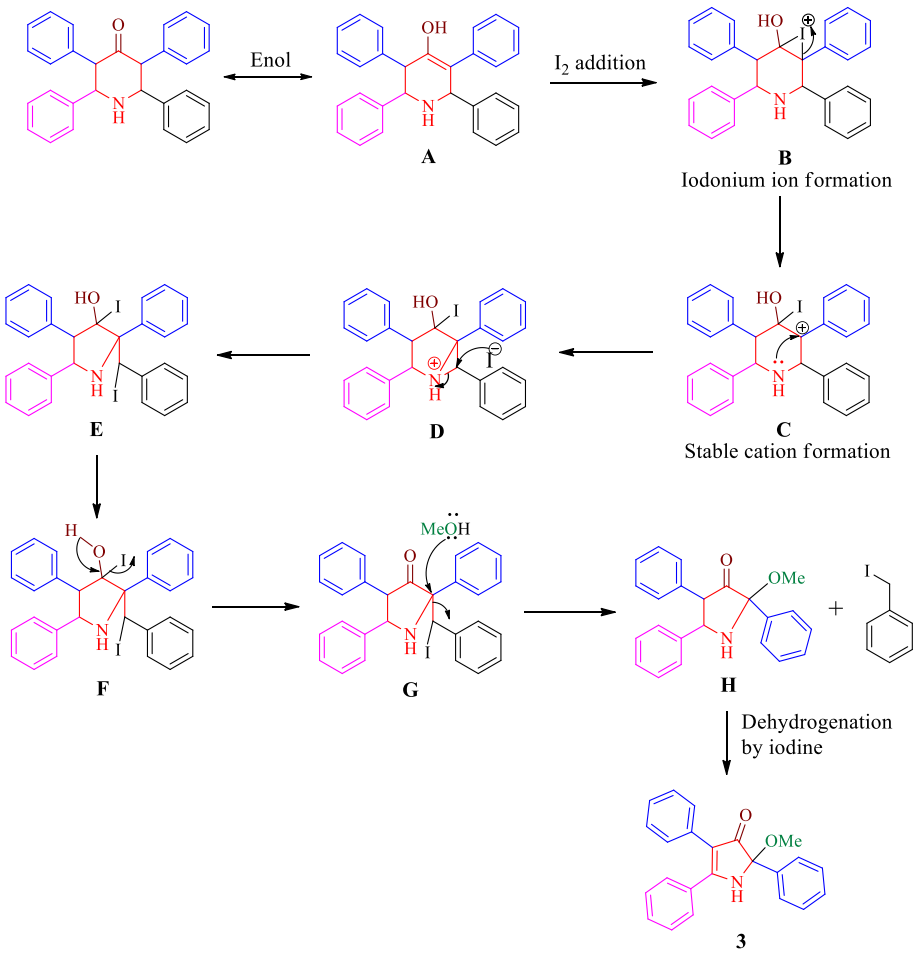

Scheme 3. Tentative mechanism.

Table 6
Antifungal activity of compounds **3a**–**3e**.

Entry	Zone of Inhibition (mm)		
	Candida albicans		
	0.5 mg/mL	1.0 mg/mL	1.5 mg/mL
3a	–	13 ± 1	13 ± 2
3b	–	12 ± 2	12 ± 2
3c	–	11 ± 2	12 ± 1
3d	–	10 ± 1	10 ± 1
3e	–	13 ± 2	14 ± 1
Control	22 ± 1	23 ± 2	25 ± 1

Control–Nystatin; Solvent–DMSO; (–) No activity; (±) Standard deviation.

Table 8
IC_{50} value for compounds **3a-3e**.

Entry	Compounds	IC_{50} Value (X 10^{-4}) M
1	**3a**	1.10
2	**3b**	1.04
3	**3c**	1.04
4	**3d**	1.04
5	**3e**	1.04
6	Ascorbic acid	0.97

Table 7
Antibacterial activities of compounds **3a**–**3e**.

Entry	Zone of Inhibition (mm)											
	Gram + ve									Gram –ve		
	Staphylococcus aureus			*Bacillus cereus*			*Enterococcus faecalis*			*Klebsiella pneumoniae*		
	0.5 mg/mL	**1.0 mg/mL**	**1.5 mg/mL**	**0.5 mg/mL**	**1.0 mg/mL**	**1.5 mg/mL**	**0.5 mg/mL**	**1.0 mg/mL**	**1.5 mg/mL**	**0.5 mg/mL**	**1.0 mg/mL**	**1.5 mg/mL**
3a	–	–	–	–	10 ± 1	15 ± 1	–	–	–	10 ± 2	12 ± 1	14 ± 1
3b	–	–	–	–	11 ± 1	12 ± 1	–	–	–	12 ± 1	14 ± 2	16 ± 1
3c	–	10 ± 1	11 ± 2	–	12 ± 2	15 ± 2	–	–	–	10 ± 1	12 ± 2	14 ± 1
3d	–	–	–	–	12 ± 1	13 ± 1	–	–	–	12 ± 2	15 ± 2	16 ± 2
3e	–	14 ± 1	14 ± 1	–	14 ± 2	16 ± 2	–	11 ± 1	12 ± 1	10 ± 1	12 ± 1	14 ± 2
Control	12 ± 2	14 ± 1	15 ± 1	14 ± 1	15 ± 1	17 ± 2	21 ± 1	23 ± 2	24 ± 1	13 ± 1	15 ± 1	16 ± 2

Control–Streptomycin; Solvent–DMSO; (–) No activity; (±) Standard deviation.

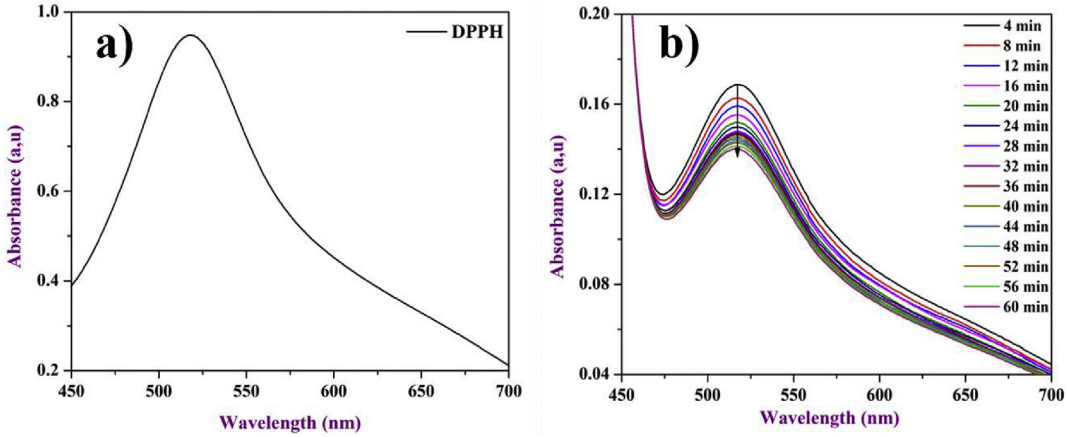

Fig. 10. Kinetic study for DPPH Vs compound **3e**: **a)** DPPH **b) 3e**.

presented in Table 6. At lower concentrations of the compounds (**3a-e**; 0.5mg/mL), there was no activity but at higher concentrations (1.0 and 1.5 mg/mL) moderate activity has been exhibited. The F/Cl substituted compounds exhibit slightly more activity compared to other compounds.

3.4.2. Antibacterial activity

The compounds **3a**–**3e** were screened for their antibacterial activities at three different concentrations of 0.5, 1.0 and 1.5 mg/mL and the results are shown in Table 7. The data reveal that the Gram-negative bacteria are more susceptible towards the tested compounds than the Gram-positive ones. In *Bacillus cereus* pathogens, compounds with electron withdrawing groups (**3c** and **3e)** exhibit slightly higher activity compared to compounds with electron donating groups (**3b** and **3d)**. In *Staphylococcus aureus* and *Enterococcus faecalis*, compounds **3c** and **3e** display good activity. All the compounds exhibit good activity against Gram-negative pathogen (*Klebsiella pneumoniae*). Compounds **3c** and **3e** display higher activity than the other compounds.

3.4.3. Antioxidant activity

The antioxidant behavior of the synthesized compounds has been determined using the modified Brand-Williams method [36]. The radical scavenging activity against 1,1-diphenyl-2-picrylhydrazyl (DPPH) is the most commonly used method for ascertaining the antioxidant activity of a compound [37]. The analyzing sample capable of donating electrons/hydrogen atoms can turn the purple color of the solution to yellow [38]. The compounds **3a-3**e were evaluated for their free radical scavenging phenomenon with ascorbic acid as the standard compound. Freshly prepared DPPH solution (1 ml in ethanol) added to 5 mL of various concentrations (2×10^{-4}, 4×10^{-4}, 6×10^{-4}, 8×10^{-4}, 10×10^{-4} M) of test compounds. After 30 min incubation period at room temperature, the absorbance was recorded at 517 nm. The IC_{50} values were calculated for the tested compounds and ascorbic acid and are summarized in Table 8 (see supplementary material for figures). The effect of the radical scavenging is increased with the increasing concentrations of the tested compounds. A lower IC_{50} value indicates a good antioxidant activity. The kinetic study was performed for the compound **3e** to verify the quenching time for DPPH radicals as shown in Fig. 10. As time increases, the intensity at 517 nm decreases indicating the quenching ability of the studied compounds.

4. Conclusion

The ring contraction and rearrangement involving tetraarylpiperidin-4-ones to 2-methoxy-2,4,5-triaryl-1H-pyrrole-3-ones is reported. A tentative mechanism for the rearrangement is proposed. The reaction conditions are mild and good yields are obtained in the reaction. Synthesized compounds exhibit significant antimicrobial, antifungal and antioxidant properties.

Acknowledgment

The authors thank the UGC, New Delhi for Major Research Project (grant No. 42–358/2013 (SR)) & UGC-Special Assistance Program (SAP). The authors gratefully acknowledge DST- FIST NMR facility of Department of Chemistry, Gandhigram Rural Institute (Deemed to be University) for the NMR spectra. S. M acknowledges CSIR, New Delhi for the award of Emeritus Scientist Scheme (Grant No. 21(1030)/16/EMR-II).

Appendix A. Supplementary data

Supplementary data to this article can be found online at https://doi.org/10.1016/j.molstruc.2019.126980.

References

[1] L. Yang, X. Shi, B.-Q. Hu, Li-Xia Wang, Iodine-Catalyzed oxidative benzylic C-H bond amination of azaarenes: practical synthesis of quinazolin-4(3*H*)-ones, Asian J. Org. Chem. 5 (2016) 494–498. https://doi.org/10.1002/ajoc.201600041.

[2] M. Jereb, D. Vrazic, M. Zupan, Iodine-catalyzed transformation of molecules containing oxygen functional groups, Tetrahedron 67 (2011) 1355–1387. https://doi.org/10.1016/j.tet.2010.11.086.

[3] P. Finkbeiner, B.J. Nachtsheim, Review iodine in modern oxidation catalysis, Synthesis 45 (2013) 979–999. https://doi.org/10.1055/s-0032-1318330.

[4] S.K. Wang, M.T. Chen, D.Y. Zhao, X. You, Q.L. Luo, Iodine-Catalyzed oxidative aromatization: a metal-free concise approach to meta-substituted phenols from cyclohex-2-enones, Adv. Synth. Catal. 358 (2014) 2093–4099. https://doi.org/10.1002/adsc.201600930.

[5] M.J. Mphahlele, F.K. Mogamisi, M. Tsanwani, S.M. Hlatshwayo, R.M. Mampa, Iodine–Methanol-promoted oxidation of 2-Aryl-1,2,3,4-tetrahydro-4-quinolones to 2-Aryl-4-methoxyquinolines, J. Chem. Research (S) (1999) 706–707. https://doi.org/10.1039/A906306D.

[6] H.G. Bonacorso, J. Navarini, C.W. Wiethan, A.F. Junges, S. Cavinatto, R. Andrighetto, M.A.P. Martins, N. Zanatta, Efficient entry to trifluoromethyl substituted chromanes from oxidative aromatization of tetrahydro-2H-chromen-5(6H)-ones using iodine/alcohol with conventional and microwave methods, J. Fluorine Chem. 142 (2012) 90–95. https://doi.org/10.1016/j.jfluchem.2012.06.024.

[7] J.S. Yadav, B.V. Subba Reddy, G. Sabitha, G.S. Kiran Kumar Reddy, Aromatization of hantzsch 1,4-dihydropyridines with I_2-MeOH, Synthesis 11 (2000) 1532–1534. https://doi.org/10.1055/s-2000-7613.

[8] M.J. Mphahlele, F.A. Oyeyiola, SuzukieMiyaura cross-coupling of 2-aryl-6,8-dibromo-1,2,3,4-tetrahydroquinolin-4-ones and subsequent dehydrogenation and oxidative aromatization of the resulting 2,6,8-triaryl-1,2,3,4-tetrahydroquinolin-4-ones, Tetrahedron 67 (2011) 6819–6825. https://doi.org/10.1016/j.tet.2011.06.085.
[9] B. Zeynizadeh, K.A. Dilmaghani, A. Roozijoy, Aromatization of hantzsch ester 1,4-dihydropyridines with iodine under normal conditions and ultrasound irradiation, J. Chin. Chem. Soc. 52 (2005) 1001–1004. https://doi.org/10.1002/jccs.200500139.
[10] V. Domingo, C. Prieto, L. Silva, J.M.L. Rodilla, J. Quílez del Moral, A.F. Barrero, Iodine, a mild reagent for the aromatization of terpenoids, J. Nat. Prod. 79 (2016) 831–837. https://doi.org/10.1021/acs.jnatprod.5b00914.
[11] R.A. Kumar, G. Saidulu, K.R. Prasad, G.S. Kumar, B. Sridhar, K.R. Reddy, Transition metal-free α-C(sp3)H bond functionalization of amines by oxidative cross dehydrogenative coupling reaction: simple and direct access to C-4-Alkylated 3,4-dihydroquinazoline derivatives, Adv. Synth. Catal. 354 (2012) 2985–2991. https://doi.org/10.1002/adsc.201200679.
[12] W. Wei, C. Zhang, Y. Xu, X. Wan, Synthesis of tert-butyl peresters from aldehydes by Bu4NI-catalyzed metal-free oxidation and its combination with the Kharasch–Sosnovsky reaction, Chem. Commun. 47 (2011) 10827–10829. https://doi.org/10.1039/C1CC14602E.
[13] J. Xie, H. Jiang, Y. Cheng, C. Zhu, Metal-free, organocatalytic cascade formation of C–N and C–O bonds through dual sp3 C–H activation: oxidative synthesis of oxazole derivatives, Chem. Commun. 48 (2012) 979–981. https://doi.org/10.1039/C2CC15813B.
[14] T. Froehr, C.P. Sindlinger, U. Kloeckner, P. Finkbeiner, B.J. Nachtsheim, A metal-free amination of benzoxazoles-the first example of an iodide-catalyzed oxidative amination of heteroarenes, Org. Lett. 13 (2011) 3754–3757. https://doi.org/10.1021/ol201439t.
[15] Z. Liu, J. Zhang, S. Chen, E. Shi, Y. Xu, X. Wan, Cross coupling of acyl and aminyl radicals: direct synthesis of amides catalyzed by Bu_4NI with TBHP as an oxidant, Angew. Chem. Int. Ed. 51 (2012) 3231–3235. https://doi.org/10.1002/anie.201108763.
[16] A. Mariappan, K. Rajaguru, N. Merukan Chola, S. Muthusubramanian, N. Bhuvanesh, Hypervalent iodine(III) mediated synthesis of 3-substituted 5-Amino-1,2,4-thiadiazoles through intramolecular oxidative S–N bond formation, J. Org. Chem. 81 (2016) 6573–6579. https://doi.org/10.1021/acs.joc.6b01199.
[17] A.T. Khan, A. Ghosh, M.M. Khan, One-pot four-component domino reaction for the synthesis of substituted dihydro-2-oxypyrrole catalyzed by molecular iodine, Tetrahedron Lett. 53 (2012) 2622–2626. https://doi.org/10.1016/j.tetlet.2012.03.046.
[18] V. Kavala, C. Lin, C.W. Kuo, H. Fang, C.F. Yao, Iodine catalyzed one-pot synthesis of flavanone and tetrahydropyrimidine derivatives via Mannich type reaction, Tetrahedron 68 (2012) 1321–1329. https://doi.org/10.1016/j.tet.2011.11.022.
[19] A. Arcadi, S. Cacchi, S. Di Giuseppe, G. Fabrizi, F. Marinelli, Electrophilic cyclization of o-acetoxyand o-benzyloxyalkynylpyridines: an easy entry into 2,3-disubstituted furopyridines, Org. Lett. 4 (2002) 2409–2412. https://doi.org/10.1021/ol0261581.
[20] G. Vengatesh, M. Sundaravadivelu, Quantum Chemical, Experimental, Theoretical Spectral (FT-IR and NMR) Studies and Molecular Docking Investigation of 4,8,9,10-Tetraaryl-1,3-Diazaadamantan-6-Ones, Research on Chemical Intermediates, 2019. https://doi.org/10.1007/s11164-019-03838-9.
[21] P. Goel, O. Alam, M.J. Naim, F. Nawaz, M. Iqbal, M.I. Alam, Eur. J. Med. Chem. 157 (2018) 480. https://doi.org/10.1016/j.ejmech.2018.08.017.
[22] Bartlomiej Sadowski, Khaled Hassanein, Barbara Ventura, Daniel T. Gryko, Tetraphenylethylenepyrrolo[3,2-b]pyrrole hybrids as solid-state emitters: the role of substitution pattern, Org. Lett. 20 (2018) 3183–3186. https://doi.org/10.1021/acs.orglett.8b01011.
[23] V. Cadierno, P. Crochet, Ruthenium-Catalyzed furan- and pyrrole-ring formation, Curr. Org. Synth. 5 (2008) 343–364. https://doi.org/10.2174/157017908786241590.
[24] A. Alizadeh, A. Rezvanian, L.-G. Zhu, One-pot synthesis of 4,5-dihydro-1H-pyrrol-3-carboxamide derivatives via a four-component reaction, Tetrahedron 64 (2008) 351–355. https://doi.org/10.1016/j.tet.2007.10.098.
[25] S.S. Basha, P. Ramachandra Reddy, A. Padmaja, V. Padmavathi, K.C. Mouli, T. Vijaya, Synthesis and antimicrobial activity of 3-aroyl-4-heteroaryl pyrroles and pyrazoles, Med. Chem. Res. 24 (2015) 954–964. https://doi.org/10.1007/s00044-014-1169-8.
[26] X.Y. He, L. Lu, J. Qiu, P. Zou, F. Yu, X.K. Jiang, L. Li, S. Jiang, S. Liu, L. Xie, Small molecule fusion inhibitors: design, synthesis and biological evaluation of (Z)-3-(5- (3-benzyl-4-oxo-2-thioxothiazolidinylidene)methyl)-N-(3-carboxy-4-hydroxy)phenyl-2,5- dimethylpyrroles and related derivatives targeting HIV-1 gp41, Bioorg. Med. Chem. 21 (2013) 7539–7548. https://doi.org/10.1016/j.bmc.2013.04.046.
[27] M. Wang, C. Ye, M. Liu, Z. Wu, L. Li, C. Wang, X. Liu, H. Guo, Synthesis and antitumor activity of 5-(5-halogenated-2-oxo-1Hpyrrolo[2,3-b]pyridin-(3Z)-ylidenemethyl)-2,4-dimethyl-1H-pyrrole3-carboxamides, Bioorg. Med. Chem. Lett 25 (2015) 2782–2787. https://doi.org/10.1016/j.bmcl.2015.05.017.
[28] C. Da, N. Telang, P. Barelli, X. Jia, J.T. Gupton, S.L. Mooberry, G.E. Kellogg, Pyrrole-Based antitubulin agents: two distinct binding modalities are predicted for C-2 analogues in the colchicine site, ACS Med. Chem. Lett. 3 (2012) 53–57. https://doi.org/10.1021/ml200217u.
[29] D.T. Mahajan, V.H. Masand, K.N. Patil, T.B. Hadda, V. Rastija, Integrating GUSAR and QSAR analyses for antimalarial activity of synthetic prodiginines against multi drug resistant strain, Med. Chem. Res. 22 (2013) 2284–2292. https://doi.org/10.1007/s00044-012-0223-7.
[30] I.S. Williams, P. Joshi, L. Gatchie, M. Sharma, N.K. Satti, R.A. Vishwakarma, B. Chaudhuri, S.B. Bharate, Synthesis and biological evaluation of pyrrole-based chalcones as CYP1 enzyme inhibitors, for possible prevention of cancer and overcoming cisplatin resistance, Bioorg. Med. Chem. Lett 27 (2017) 3683–3687. https://doi.org/10.1016/j.bmcl.2017.07.010.
[31] J.S. Moreno, D. Agas, M.G. Sabbieti, M.D. Magno, A. Migliorini, M.A. Loreto, Synthesis of novel pyrrolyl-indomethacin derivatives, Eur. J. Med. Chem. 57 (2012) 391–397. https://doi.org/10.1016/j.ejmech.2012.09.008.
[32] L. Dyson, A.D. Wright, K.A. Young, J.A. Sakoff, A. McCluskey, Synthesis and anticancer activity of focused compound libraries from the natural product lead, oroidin, Bioorg. Med. Chem. 22 (2014) 1690–1699. https://doi.org/10.1016/j.bmc.2014.01.021.
[33] M.C. Etter, J.C. MacDonald, J. Bernstein, Graph-set analysis of hydrogen-bond patterns in organic crystals, Acta Crystallogr. B46 (1990) 256–262. https://doi.org/10.1107/S0108768189012929.
[34] F.L. Hirshfeld, Bonded-atom fragments for describing molecular charge densities, Theor. Chim. Acta 44 (1977) 129–138. https://doi.org/10.1007/BF00549096.
[35] M.J. Turner, J.J. MacKinnon, S.K. Wolff, D.J. Grimwood, P.R. Spackman, D. Jayatilaka, M.A. Spackman, Crystal Explorer, University of Western, Australia, 2017.
[36] W. Brand-Williams, M.E. Cuvelier, C. Berset, Use of a free radical method to evaluate antioxidant activity, Food Sci. Technol. Lett. 28 (1995) 25–30. https://doi.org/10.1016/S0023-6438(95)80008-5.
[37] M. Burits, F. Bucar, Antioxidant activity of *Nigella sativa* essential oil, Phytother Res. 14 (2000) 323–328. https://doi.org/10.1002/1099-1573(200008)14:5%3c323::AID-PTR621%3e3.0.CO;2-Q.
[38] M.Z. Gul, F. Ahmad, A.K. Kondapi, I.A. Qureshi, I.A. Ghazi, Antioxidant and antiproliferative activities of *Abrus precatorius* leaf extracts - an *in vitro* study, BMC Complement Altern. Med. 13 (2013) 1–12. https://doi.org/10.1186/1472-6882-13-53.